Final Report

May 2002

Simon J. Hook
Fred J. Prata
Geoffrey S. Schladow

(http://shookweb.jpl.nasa.gov/validation)
(http://laketahoe.jpl.nasa.gov)

Table of Contents

Summary 5
1.0 Introduction 7
2.0 Site Selection Criteria 8
3.0 Site Descriptions and Status 9
3.1 Lake Tahoe CA/NV 9
3.2 Australian Sites 11
4.0 Methodology 15
4.1 Validation of In-flight Radiometric Calibration of Products AST01B and MOD02 15
4.2 Error Analysis of Procedure for Validation of In-Flight Radiometric Calibration. 15
4.3 Validation of Surface Radiance, Temperature and Emissivity Products AST05, AST08 and MOD11 17
4.4 Error Analysis of Procedure for Surface Radiance, Temperature and Emissivity Product Validation 18
5.0 The JPL Calibration and Computing Facilities 18
6.0 Current Results 19
6.1 Validation of At Sensor Radiance Product from ASTER and MODIS 19
6.2 Validation of Surface Products from ASTER and MODIS 22
Publications and Media (this project) 28
References 29
Collaborations 31
Archiving 31
WebPages 31

List of Figures

Figure 1 Bathymetric map of Lake Tahoe with a contour interval of 50 m. The 4 NASA buoys are labeled TB1, TB2, TB3 and TB4. Also shown is the US Coast Guard station (USCG), Midlake (MLTP) and Index (LTP) stations. Additional rafts deployed by UCD on a semi-permanent basis are labeled TDR1 and TDR2..... 9
Figure 2 Surface monitoring station at TB4. 10
Figure 3 Location of the CIGSN sites..... 12
Figure 4 Brightness temperature variation as a function of zenith angle at different times of day. 14
Figure 5 MODIS Terra % Radiance Difference between Vicarious and OBC Derived Radiance for Channel 31 at Lake Tahoe CY2000-2002 ((V-O)/V)*100 20
Figure 6 ASTER 3x3 pixel % Radiance Difference between Vicarious and OBC Derived ((V-O)/V)*100. 21
Figure 7 Differences between ASTER Products (AST1B, AST08) and Vicarious Measurements at Lake Tahoe CA/NV CY 2000-2002 23
Figure 8 Daytime MODIS scene acquired over Lake Tahoe on 3/12/2000. Image on left is a grayscale brightness temperature image from the band 31 and image on right is the MODIS surface temperature product. 24
Figure 9 Difference between MODIS LST (MOD11) and Vicarious Measurements at Lake Tahoe CA/NV CY 2000-2002 25
Figure 10 Left image – Cloud Mask for Uardry region using Collection 3 software. Pixels colored green were identified as 99% cloud-free by the cloud mask algorithm and processed to surface temperature. Cloud Mask for Uardry region (same input scene as left image) processed using the Collection 4 software. 26
Figure 11 Change in emissivity over time at the Uardy site. 27
Figure 12 Change in emissivity at the Amburla site. 27

List of Tables

Table 1 Measurements made at Lake Tahoe site. LR – Longwave Radiation (↑-up, ↓-down), SR – Shortwave Radiation (↑-up, ↓-down), NR – Net Radiation, v – Wind Speed, WD – Wind Direction, Ps – Pressure, AOD - Aerosol Optical Depth, ToV - Total Column Water, TSI - Total Sky Imager, Ta – air temperature, Ts – Radiometer skin temp., Tb - Bulk temp. 11
Table 2 Measurements made at the Uardry field site (near Hay) and their locations. Tg is ground temperature, see Table 1 for explanation of other symbols. 13
Table 3 Locations and measurements available at the Amburla field site. Tg is ground temperature, see Table 1 for explanation of other symbols. 14
Table 4 Locations and measurements available at the Thangoo field site. Tg is ground temperature, see Table 1 for explanation of other symbols. 15
Table 5 Sensitivity Analysis of the Effect of Errors in the Atmospheric Profile on the Correction for Reflected Downwelling Radiation with the Radiometer data at the Tahoe Site. 16

Table 6 Change in MODIS Radiance and Brightness Temperature at Sensor for Various Atmospheric Perturbations at the Tahoe Site..... 17
Table 7 Summary Validation Results for the In-Flight Validation of Absolute Calibration of MODIS and ASTER "Window" TIR Channels (T=Terra ; A=Aqua) 22
Table 8 Average bias Between Instrument Derived Surface Temperature and Measured Surface Temperature for the Uardry Field Site..... 26

Summary

The objective of this study was to validate the thermal infrared data and products acquired over land from the Advanced Spaceborne Thermal Emission and Reflectance Radiometer (ASTER) and the Moderate Resolution Imaging Spectroradiometer (MODIS) using a set of automated validation sites. The main advantage of this approach as compared to the approach of conducting periodic in-flight validation experiments is the necessary data are acquired automatically allowing validation whenever satellite data are available. Four automated validations sites were established as part of the study, which are located at L. Tahoe, CA/NV, USA; Thangoo, WA, Australia; Amburla, NT, Australia and Uardry, NSW, Australia. The sites were chosen to encompass a range of cover types and atmospheric conditions. At each site, all the instrumentation necessary to validate the products of interest was deployed including one or more custom self-calibrating highly accurate radiometers. The Lake Tahoe site was chosen to enable validation of both the radiance at sensor and the surface products (radiance, temperature and emissivity) whereas the Australian sites were chosen to only validate the surface products.

Results from the Lake Tahoe site indicate the accuracy of the thermal infrared radiance measured by the MODIS instruments on both the Terra and Aqua satellites has met or exceeded the preflight specification from launch through 2002. In comparison the radiance measured by the ASTER instrument met specification in the early part of the mission but failed to meet specification late in 2002 with biases slightly larger than 1K. The biases resulted from instrument drift, which was measured, but the corrections for the drift were not implemented with sufficient frequency in the Level 1 software to correct the problem. The ASTER science team is in the process of providing a web-based tool for users to determine the size of the correction so users can implement their own correction. Analysis of the surface products (radiance, temperature, emissivity) at the Lake Tahoe site indicate both the ASTER and MODIS land surface temperature products have small biases but are within the 1K accuracy specification, provided the initial instrument measured radiance is correct. If there is a bias in the initial ASTER radiance, a temperature equivalent error is added to the surface temperature product. In the case where the instrument data is well calibrated the MODIS product has a slight positive bias (satellite derived minus ground measured) whereas the ASTER product has a negative bias (satellite derived minus ground measured).

Validation of the ground products at the Australian sites is inherently more difficult because the surface is less homogenous and the atmosphere contains more water vapor. However, since the accuracy of the ground products is cover type dependant, it is essential the products be validated over a range of cover types. Comparisons at the Australian sites indicate the ASTER and MODIS products do not meet specification with an average bias from launch through 2002 of ~ 2K. Generally the bias associated with the ASTER product is smaller than the MODIS product. The smaller bias of the ASTER product is thought to be due to the ability of the ASTER algorithm to compensate for natural changes in site emissivity over time compared to the MODIS algorithm, which assumes the site emissivity, is fixed.

It is essential that the ASTER and MODIS products continue to be validated to guarantee the products meet the accuracy and precision requirements over the entire mission and are suitable as Climate Data Records (CDR's). The CDR's would provide a continuous record from the start of EOS through the launch of NPOESS. Continued validation is also particularly important for ASTER to make sure any corrections to compensate for the instrument degradation are valid.

Data from the sites have also been used to help identify problems with the input products such as the MODIS cloud mask product as well as validate data from other instruments such as Landsat 5 and ETM+. In the case of ETM+ the data have been used to help correct a large instrument bias identified in the early part of the mission. Further work is required to correct a similar problem with Landsat 5 data.

1.0 Introduction

In-flight validation of thermal infrared data acquired by satellites and aircraft has long been recognized as an essential method to ensure their accuracy and precision. Several authors have conducted experiments to determine in-flight spectral and radiometric calibration of thermal infrared scanners mounted on aircraft and spacecraft (e.g Schott and Volchok, 1985; Prata, 1994; Hook and Okada 1996; Wan et al. 2002, Barsi et al. 2003, Hook et al. 2003).

These experiments typically involve independently measuring the radiance emitted by the surface in the thermal infrared and also the properties of the atmosphere above the surface and then inputting these data into a radiative transfer model to predict the at-sensor radiance. The predicted at-sensor radiance is then compared to the radiance at-sensor measured by the satellite or aircraft instrument. This approach is often referred to as the ground-based radiance method and is used in this study. Further details on this approach are presented in subsequent sections. A second approach is to acquire data simultaneously with the satellite overpass from a well characterized thermal infrared sensor mounted on an aircraft, and then propagate the aircraft radiance through a radiative transfer model to predict the radiance at the satellite. This approach is referred to as the aircraft radiance method. Both of these methods are loosely referred to as vicarious calibration.

The primary disadvantage of the ground-based method is its dependency on the radiative transfer model. This is the primary advantage of the airborne method since additional modification of the aircraft radiance to satellite altitudes is minimized because one of the primary contributors to the at-sensor radiance is atmospheric water vapor, most of which is typically beneath the aircraft. The primary disadvantage is the calibration of the aircraft instrument may not be sufficiently well known.

In previous studies, the approach taken to validation has typically involved periodic validation campaigns where all the necessary validation measurements are made at the time of the satellite overpass. This approach works well for identifying anomalous behavior, but it is difficult to conduct the campaigns with sufficient frequency to monitor gradual changes over long periods of time. An alternative approach involves the development of long-term automated sites where all the necessary validation measurements are made on a continuous basis. This latter approach was proposed to the NASA Research Announcement on “Satellite Remote Sensing Measurement Accuracy, Variability, and Validation Studies” for the validation of ASTER and MODIS data. The proposal was accepted and four automated validation sites were established to validate the thermal infrared data and products from MODIS and ASTER. The four sites are located at L. Tahoe, CA/NV, USA; Thangoo, WA, Australia; Amburla, NT, Australia and Uardry, NSW, Australia. The sites were chosen to encompass a range of cover types and atmospheric conditions.

The subsequent sections of this report describe each of the sites and summarize the results from the validation of the ASTER and MODIS products at the sites. The report is

divided into the following main sections: Site Selection Critera, Site Descriptions and Status, Methodology, Calibration Facilities, Current Results, Publications and Media, References, Collaborations, Archiving, Web Pages and References. The Site Selection Criteria section explains why these particular sites were chosen. The Site Descriptions and Status section provides a brief physical description of the sites, the measurements made at the sites and the status of each site. The Methodology section describes the procedure used to validate the products as well an analysis of any errors associated with the procedure. The Calibration facilities section describes the procedure used to validate certain critical field equipment and the Current Results section provides an in depth discussion of the validation results. The final few sections provide additional information on publications, collaborations, data archiving and data sources.

2.0 Site Selection Criteria

The objective of this study was to validate the thermal infrared data and products from ASTER and MODIS. These include the radiance at sensor, surface radiance, surface temperature and surface emissivity.

In order to validate the **radiance at sensor** a ground site should meet the following criteria:

1) Homogenous at scales appropriate for validating the instrument of interest. Since the ASTER and MODIS TIR bands have nadir spatial resolutions of ~90 m and ~ 1 km respectively then the target should be homogenous at scales from 10's of m's to a few km's.
2) Low water vapor loadings. In the forward calculation, incorrect knowledge of the amount of water vapor in the atmosphere can result in a large error and therefore sites with low amounts of water vapor are desirable.
3) Wide temperature range.

The Lake Tahoe site was selected to validate the **radiance at sensor** since it met the above criteria, in addition the site is fairly accessible for instrument maintenance and since the lake is freshwater there is no damage to instrumentation due to salt.

In order to validate the surface products (**radiance at surface**, **surface temperature, surface emissivity)** multiple ground sites are required which should meet the following criteria:

1) Homogenous at scales appropriate for validating the instrument of interest.
2) A range of water vapor loadings so the algorithms for retrieving the geophysical variables can be tested for a variety of atmospheric conditions.
3) A range in temperatures and emissivities so the algorithms can be evaluated over different cover types.

The Lake Tahoe site ***and*** the Australian sites were selected to meet these criteria. The Australian sites include a grassland site (Uardry), a bare soil site (Amburla) and an open

woodland site (Thangoo). Together the sites include a wide range in water vapor, emissivity and temperature allowing good validation statistics to be generated for the surface products.

3.0 Site Descriptions and Status

3.1 Lake Tahoe CA/NV

Lake Tahoe is a large lake situated in a granite graben near the crest of the Sierra Nevada Mountains on the California - Nevada border, at 39° N, 120° W. It is the 11th deepest lake in the world and due to its large thermal mass, does not freeze in winter.

The Jet Propulsion Laboratory (JPL) and UC Davis (UCD) are currently maintaining four surface sampling stations on Lake Tahoe together with instrumentation onshore. The following description of the measurements at the site is summarized from Hook et al. (2003). The four surface sampling stations are referred to as TB1, TB2, TB3 and TB4 (Figure 1). They are deployed sufficiently distant from each other to enable validation of 4 separate pixels from a sensor with a 1 km spatial resolution. Each station has a single JPL-built self-calibrating near nulling radiometer measuring the skin temperature from a height of 1m and several bulk temperature sensors, placed 2 cm beneath the surface (Figure 2).

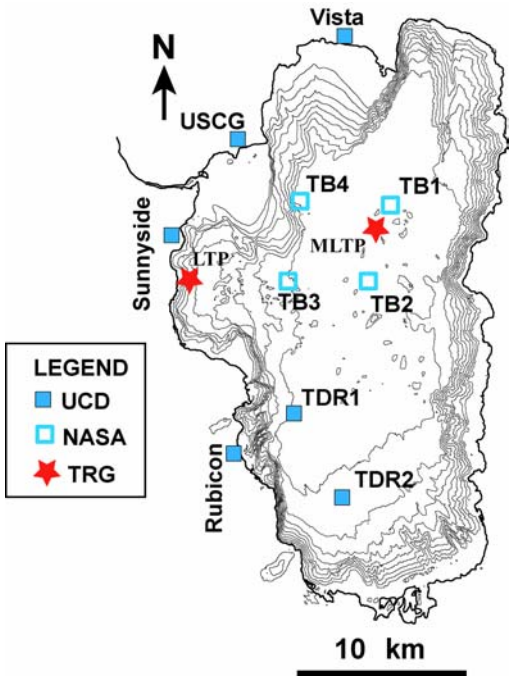

Figure 1 Bathymetric map of Lake Tahoe with a contour interval of 50 m. The 4 NASA buoys are labeled TB1, TB2, TB3 and TB4. Also shown is the US Coast Guard station (USCG), Midlake (MLTP) and Index (LTP) stations. Additional rafts deployed by UCD on a semi-permanent basis are labeled TDR1 and TDR2.

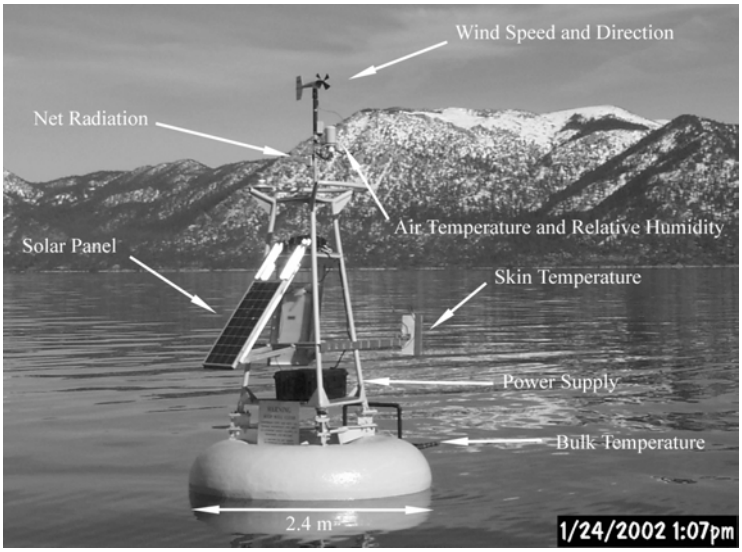

Figure 2 Surface monitoring station at TB4.

The JPL radiometer has an accuracy of ± 0.1 K which was confirmed in a recent cross comparison experiment with several other highly accurate radiometers in both a sea trial and in laboratory comparisons (Barton et al. 2002). A comparison of the JPL radiometer, against the Marine Atmospheric Emission Radiance Interferometer (MAERI), a recognized standard within the sea surface temperature community over a 1.5 day cruise indicated the JPL radiometer agreed with the MAERI to 0.007 K.

The bulk water temperature is measured with several temperature sensors mounted on a float tethered behind the raft (Figure 2). Multiple temperature sensors are used to enable cross verification and each float has up to 12 temperature sensors all at ~ 2cm beneath the surface. The temperature sensors used have a calibration accuracy of ± 0.10 °C. The temperature sensors and radiometers are calibrated in the JPL NIST Traceable Calibration Facility. The procedure for calibrating the temperature sensors and radiometers at the facility is described later. A full set of measurements is made every 2 minutes and data are downloaded daily by cellular telephone modem. A meteorological station (wind speed, wind direction, air temperature, relative humidity and net radiation) is also deployed on each buoy (Figure 2). It should be noted that the bulk temperature, measured by the temperature sensors beneath the surface is not the same as the skin temperature measured by the radiometer. The skin temperature is typically 0.5 ° C cooler than the bulk temperature due to convective cooling of the surface but can be as much as a 1 ° C cooler or warmer than the skin temperature depending on the conditions. The satellite sensor measures the skin temperature and therefore it is essential that the site use radiometers and bulk temperature measurements to validate the satellite radiance. Since the Tahoe buoys continuously measure both the skin and bulk temperature they also provide a useful dataset for the analysis of the difference between skin and bulk temperatures and the relationship between these temperatures and the air-lake heat flux.

Both JPL and UCD maintain additional equipment at the US Coast Guard station including a full meteorological station (wind speed, wind direction, air temperature, and

relative humidity), full radiation station (long and shortwave radiation up and down), a shadow band radiometer and an all sky camera. The shadow band radiometer provides information on total water vapor and aerosol optical depth. The UCD also maintains two long-term monitoring stations on the lake referred to as Index and MidLake (Figure 1). Measurements are made at these stations approximately every 10 days and include profiles of algal growth rate using 14C, nutrients (N, P), chlorophyll, phytoplankton, zooplankton, light, temperature and secchi disk transparency.

Atmospheric profiles for the site are obtained from both local sounding balloon launches model data generated by the National Center for Environmental Prediction (NCEP). The NCEP produces global model values on a 1-degree by 1-degree grid at 6 hr intervals. Lake Tahoe is on a grid point and the NCEP data are interpolated to the overpass time. The location and types of measurements made at the Tahoe site are summarized in Table 1.

Table 1 Measurements made at Lake Tahoe site. LR – Longwave Radiation (↑-up, ↓-down), SR – Shortwave Radiation (↑-up, ↓-down), NR – Net Radiation, v – Wind Speed, WD – Wind Direction, Ps – Pressure, AOD - Aerosol Optical Depth, ToV - Total Column Water, TSI - Total Sky Imager, Ta – air temperature, Ts – Radiometer skin temp., Tb - Bulk temp.

Map Key	Latitude (N)	Longitude (W)	Measurement
US Coast Guard	39° 10.838	120° 07.157	v, WD, Ps, LR↑, LR↓, SR↑, SR↓, AOD, ToV, TSI
TB1	39° 09.180	120° 00.020	Ts, Tb, Tb, Tb, Tb, NR, v, WD, Ps, Ta
TB2	39° 09.290	120° 00.020	Ts, Tb, Tb, Tb, Tb, NR, v, WD, Ps, Ta
TB3	39° 08.300	120° 04.920	Ts, Tb, Tb, Tb, Tb, NR, v, WD, Ps, Ta
TB4	39° 09.300	120° 04.330	Ts, Tb, Tb, Tb, Tb, NR, v, WD, Ps, Ta

On October 31st and November 1st 2002 the two southern buoys (TB3 and TB4) were relocated slightly further south in order to make all 4 buoys at least 5 km from shore. TB3 is now located at 39° 06.612, 120° 04.521 and TB4 is located at 39° 09.300, 120° 04.330.

3.2 Australian Sites

Australia's Continental Integrated Ground Site Network (CIGSN) currently has three operational sites referred to as Uardry, Amburla and Thangoo. The Uardry site is 60 km NE of the town of Hay (New South Wales). The Amburla site is 100 km WNW of Alice Springs (Northern Territory) and the Thangoo site is 40 km south of Broome (Western Australia) (Figure 3). The CIGSN is producing accurate and long time series of surface radiative fluxes and meteorological parameters such as surface temperature, air temperature, relative humidity, wind speed and surface pressure.

The measurements at the sites are recorded with an autonomous, solar-powered data collection and telemetering system purpose built for calibration and validation studies involving satellite instruments with upto kilometre-size footprints (Prata, 1994). The system operates by using RF communications with remote (or "satellite") sites that collect data (e.g. temperatures, radiation, wind speed etc.) and send these signals to a central processing unit that can log and perform intelligent software tasks.

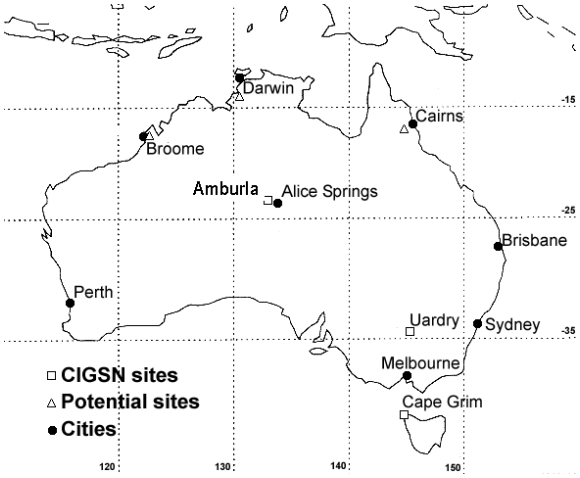

Figure 3 Location of the CIGSN sites.

3.2.1 Uardry Site, NSW

This site was established in mid-1992 and has been running continuously to the present. It is located near the center of the largest and most uniform plain on the Australian continent. The vegetation cover at the site is grassland. Atmospheric conditions are very favorable for remote sensing validation since aerosol optical depth at 550 nm rarely exceeds 0.05 and cloudiness is low. The site is arranged as a central site with 8 "satellite" sites which telemeter data to the central site up to 6 times per minute.

The central site includes a 15m tower with instruments mounted on a boom extending from the tower. A variety of measurements are made at the central site as well as the satellite sites (Table 2) including the surface temperature by both contact (transducers) and non-contact (radiometers). Over time methods have been developed to ensure correct placement of the contact sensors (upto 25 across a 1 km x 1 km area) to ensure they provide a good measure of the surface temperature over the site. The radiometers are self calibrating and were developed by the Commonwealth Scientific Industrial Research Organization (CSIRO). Three radiometers are deployed at the central site at three different zenith angles, viz. 0.0, 30.0, and 55.0; each radiometer takes 10 s samples and reports measurements every 2 minutes continuously.

Table 2 Measurements made at the Uardry field site (near Hay) and their locations. Tg is ground temperature, see Table 1 for explanation of other symbols.

Site No.	Latitude	Longitude	Parameters
00 (Central)	34°23.50'S	145°18.28'E	Tg, Tg, Tg, Tg, Ta (2 m), Ta (15 m), RH (2 m), RH (15 m), SR↑, SR↓, LR↑, LR↓, v, Ps, Ts, Ts, Ts, AOD, ToV
02 (N500)	34°23.27'S	145°18.33'E	Tg, Tg, Ta, SR↑
03 (W250)	34°23.50'S	145°18.11'E	Tg, Tg, Tg, Tg
04 (S250)	34°23.66'S	145°18.21'E	Tg, Tg, Tg, SR↑
05 (E500)	34°23.53'S	145°18.53'E	Tg, Tg, Tg, SR↑
06 (S500)	34°23.76'S	145°18.18'E	Tg, Tg, Ta, v
07 (W500)	34°23.45'S	145°17.97'E	Tg, Tg, Tg, SR↓
08 (E250)	34°23.50'S	145°18.42'E	Tg, Tg, Tg

3.2.2 Amburla, NT

The Amburla site has been providing near-continuous surface measurements since March 1995. The instrumentation is deployed on a 12 x 12 km^2 plain which is sparsely covered with grass tufts. The layout consists of a central data logging site coupled with 6 "satellite" sites. Measurements made at the site are summarized in Table 3. Several radiometers were added to the site in 2000 including a scanning radiometer. The scanning radiometer scans from –70 to +70 degrees through nadir, with one view of the sky to provide a correction for reflected sky radiation. After averaging these data over many days to remove solar heating and wind-induced thermal effects, a clear angular variation can be discerned in the nighttime data. Figure 4 below shows some results, where it can be seen that at 0200, 0600, 1800 and 2200 hours local time there is a strong variation of the brightness temperature with angle. During the day the angular variation is masked by significant differential solar heating of the surface and by shading effects. These data are useful in assessing the surface temperature and emissivity products from MODIS and ASTER at off-nadir view angles.

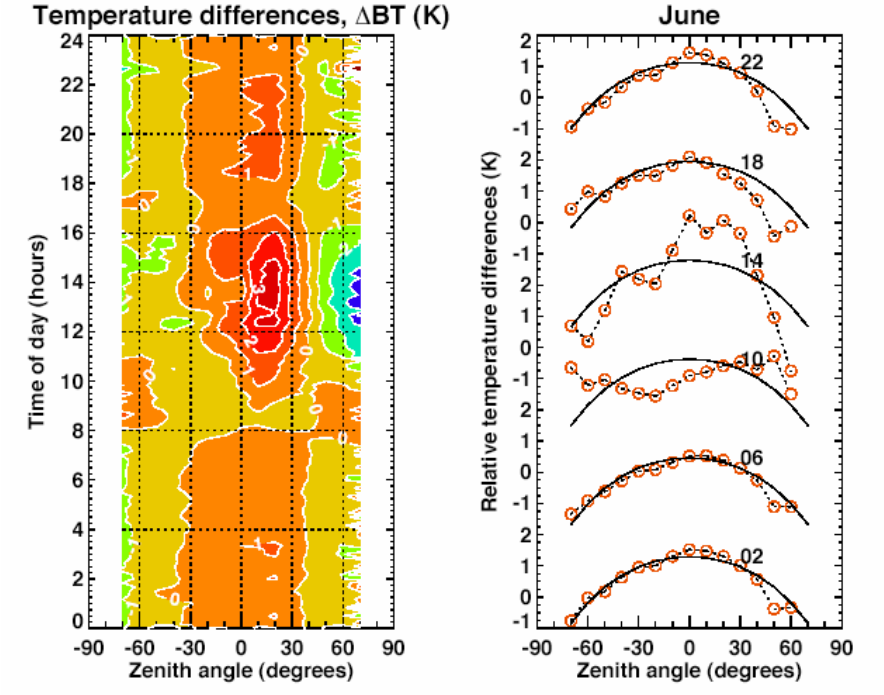

Figure 4 Brightness temperature variation as a function of zenith angle at different times of day.

Table 3 Locations and measurements available at the Amburla field site. Tg is ground temperature, see Table 1 for explanation of other symbols.

Site No	Latitude (°S)	Longitude (°E)	Parameter
00	23°22.813	133°06.788	Tg, SR↓, Ts (scan), AOD, ToV
01	23°23.415	133°07.080	Tg, Tg
02	23°23.116	133°07.136	Tg, SR↑
03	23°23.116	133°07.136	Tg, SR↑
04	23°23.116	133°07.136	Tg, Ta
05	23°22.753	133°07.239	Tg, SR↓
06	23°23.116	133°07.136	Tg, SR↓
07	23°23.116	133°07.136	Tg, Tg
08	23°23.116	133°07.136	LR↑, LR↓

3.2.3 Thangoo, WA

The Thangoo site was established in 1998. The site was chosen because it is in a monsoonal climate zone with water vapor loadings ranging from as low as 1 cm of precipitable water to values in excess of 7 cm during the wet season. In a typical year the wet season lasts from December to April. The remaining seven months are dry with the highest percentage of clear skies anywhere in Australia. The site is located in tropical

savanna woodland (Acacia). Measurements at the site are summarized in Table 4 and include four CSIRO scanning radiometers. Some ground sensors are used, but the nature of the biome make relating understory surface temperature measurements to satellite measurements impractical. The scanning radiometer measurements are made from masts 6 m high, to measure the radiation from the canopy (average height 3-4 m) and understory. Radiosonde data are available daily from Broome (Figure 3).

Table 4 Locations and measurements available at the Thangoo field site. Tg is ground temperature, see Table 1 for explanation of other symbols.

Site No	Latitude (S)	Longitude (E)	Parameter
1	18°11'02.40"S	122°22'44.93"E	Tg, Ta (1.8m agl), Ta (8m agl), Ts↑ (8m agl), AT, RH
2	18°10'59.02"S	122°23'36.06"E	Tg, Ta (1.8m agl), Ta (8m agl), Ts↓ (8m agl), AT, RH
3	18°12'24.31"S	122°24'03.90"E	Tg, Ta (1.8m agl), Ta (8m agl), Ts↓ (8m agl), AT, RH
4	18°10'52.81"S	122°21'28.20"E	Tg,Tg,Tg, Ts↑ (8m agl), AT, RH
5	18°10'52.80"S	122°21'28.30"E	v, WD, AT, RH, Ps
6	18°10'52.68"S	122°21'28.30"E	SR↑, SR↓, LR↑, LR↓

4.0 Methodology

The following section summarizes the procedures used for reducing the field data in order to compare them with the satellite data. The section also includes error analysis on certain data reduction procedures.

4.1 Validation of In-flight Radiometric Calibration of Products AST01B and MOD02

As discussed previously the water site is used to validate the in-flight radiometric calibration of the ASTER and MODIS thermal bands. The list below summarizes the procedure for validating the in-flight calibration using the water site.

- Extract the bulk temperature
- Extract the radiometric temperature.
- Correct the radiometric temperature to skin kinetic temperature.
- Propagate the skin temperature to the satellite using a radiative transfer model (MODTRAN 3.5) and interpolated atmospheric profile.
- Convolve the propagated at-sensor radiance to the instrument response function to obtain the vicarious radiance (VR).
- Extract the image radiance derived with the On Board calibrator (OBC).
- Compare and contrast the OBC and VR values.

4.2 Error Analysis of Procedure for Validation of In-Flight Radiometric Calibration

In order to validate the radiance measured by the satellite sensor it is necessary to derive the equivalent at-sensor radiance from the field radiometer measurements. There are 3 primary sources of error in deriving the at-sensor radiance from the field data at the water site. They are:

- Radiometer accuracy, precision and uncertainty.
- Correction of the radiance measured by the radiometer to kinetic temperature.
- Propagation of the kinetic temperature to the at-sensor radiance using a radiative transfer model.

The list above assumes the emissivity of the surface is known and constant which is true for a water surface when the measurements are made with a radiometer looking straight down, as is the case with the Tahoe measurements. If the radiance from the water surface is measured at off-nadir angles or at varying wind speeds, the emissivity does vary and can be determined using an emissivity model, e.g. Wu and Smith (1997). Accuracy, precision and uncertainty values for a typical JPL radiometer are 0.08, 0.03 and 0.085 respectively.

The JPL radiometer does not make a measurement of the sky temperature and therefore the contribution to the radiometer signal from the downwelling sky radiance is calculated using the MODTRAN Radiative Transfer Code (RTC) (Berk et al. 1989) and removed. The error associated with this correction was determined by running the RTC with a US standard atmosphere and calculating the downwelling radiance for the Tahoe site with the radiometer measuring a brightness temperature of 5 and 20 C, the typical minimum and maximum temperature of Lake Tahoe. The standard atmosphere was then perturbed to simulate the effect of an error in the input profile. An error of ± 10 % was assumed for the water vapor profile, an error of ± 1 C was assumed for the temperature profile and an error of ± 50 % was assumed for the ozone profile. The downwelling radiance determined from the different RTC runs was then used to correct for the reflected downwelling radiance and the effect of an error in the input profile determined (Table 5).

Table 5 Sensitivity Analysis of the Effect of Errors in the Atmospheric Profile on the Correction for Reflected Downwelling Radiation with the Radiometer data at the Tahoe Site.

Perturbation	**Kinetic Temperature (degrees C)**		**Difference from no perturbation (degrees C)**	
None	5.579	20.703	0	0
90% Water Vapor	5.585	20.707	0.006	0.004
110% Water Vapor	5.573	20.699	-0.006	-0.004
-1 deg C	5.585	20.708	0.006	0.005
+1 deg C	5.573	20.699	-0.006	-0.004
Ozone Factor 50%	5.585	20.709	0.006	0.006
Ozone factor 150%	5.574	20.700	-0.005	-0.003

In the table above the total downwelling sky corrections are 0.2 C and 0.168 C for the 5 and 20 C cases respectively. If there is an error in the knowledge of the water vapor

profile of 10 % there will be an error in the recovered temperature of 0.006 C. Smaller errors will result from an error in either the air temperature or ozone. Clearly for the JPL radiometers the effect of an error in the atmospheric profile used to correct for downwelling sky radiation is small (see Hook et al. 2003 for further details).

The third primary source of error is associated with any error in the atmospheric profile when it is used to propagate the ground radiance (calculated from the kinetic temperature derived from the radiometer and assumed emissivity for water) to the altitude of the satellite sensor. Clearly this error will vary depending on the wavelength range covered by the channel that is being studied. In order to assess this error the surface radiance was propagated to the sensor using a US standard profile and then the profile was perturbed in a similar manner to that used to assess the correction for the downwelling radiance (Table 6).

Table 6 Change in MODIS Radiance and Brightness Temperature at Sensor for Various Atmospheric Perturbations at the Tahoe Site.

Change from Nominal Brightness Temperature (degrees C)	Channel 28 (7.34 µm)	Channel 29 (8.53 µm)	Channel 30 (9.73 µm)	Channel 31 (11.01 µm)	Channel 32 (12.03 µm)	Channel 33 (13.37 µm)
90% Water Vapor	0.92	0.154	0.046	0.107	0.15	0.18
110% Water Vapor	-0.834	-0.155	-0.046	-0.107	-0.16	-0.194
-1 deg C	-0.742	-0.071	-0.305	-0.038	-0.054	-0.271
+1 deg C	0.742	0.07	0.314	0.046	0.053	0.27
50% Ozone	0	0.173	8.158	0	0.009	0.463
150% Ozone	0	-0.175	-5.461	0	-0.009	-0.439
50% Visibility (11.5 km)	0.013	0.096	0.074	0.084	0.071	0.025
150% Visibility (34.5 km)	-0.039	-0.272	-0.213	-0.246	-0.213	-0.103

The amount of water vapor in the US Standard Atmosphere is greater than is typical at Lake Tahoe (0.5-1.5 cm total column water) but because of the altitude of the site the effect for the clear window channels of MODIS (29, 31 and 32) is still small for a large error in the water vapor. For example a 10% error in the water vapor profile results in an error in the at sensor brightness temperature of 0.107 for MODIS channel 31. The size of this error would be greater for a wetter, warmer atmosphere at sea level. Although the effect of water vapor is small at Lake Tahoe every effort is made to fully characterize the atmosphere. This includes the launching of sounding balloons to obtain atmospheric profiles at the time of the overpass and monitoring the total water vapor and ozone using a shadow band radiometer as well as comparing in situ profile measurements with model profile data.

4.3 Validation of Surface Radiance, Temperature and Emissivity Products AST05, AST08 and MOD11

All four sites are used to validate the surface radiance, temperature and emissivity products (AST05, AST08, AST09T, MOD11). Details of these products are available in

the ATBD's by Gillespie et al. (1999), Palluconi et al. (1999) and Wan et al. 1999. The procedure used can be summarized as:

- Extract the radiometric temperature.
- Correct the radiometric temperature to skin kinetic temperature.
- Extract the products values (AST05, AST08, AST09T, MOD11)
- Compare and contrast the product values with the vicarious values.

4.4 Error Analysis of Procedure for Surface Radiance, Temperature and Emissivity Product Validation

For the validation of the surface radiance, temperature and emissivity the primary sources of error are:

- Radiometer accuracy, precision and uncertainty.
- Correction of the radiance measured by the radiometer to kinetic temperature.

Both these errors were assessed in section 1.7.2. However, it should be noted the error associated with the correction for downwelling radiation is larger for Australian sites since the surface emissivity is less well known, especially at the soil site (Amburla). In order to obtain the most representative emissivity, the JPL field portable micro Fourier Transform Interferometer (Hook et al. 1996) is used at each site to determine the site emissivity.

5.0 The JPL Calibration and Computing Facilities

Calibration of the radiometers and bulk temperature sensors is undertaken at JPL and the facilities are summarized below, the other equipment is calibrated by the manufacturer. The radiometers and bulk temperature sensors are calibrated using a laboratory blackbody and a temperature controlled water bath respectively. Both systems are NIST traceable. In addition, JPL has developed a portable cone blackbody for field calibration (Rice et al. 2002). The specifications for the NIST traceable laboratory cone blackbody and readout system are:

- NIST designed cone in a 44 liter temperature controlled bath. Stability at 25 C: +/- 0.0007 C (7008-IR)
- Thermistor standard probe with an accuracy specification of 0.0015 ° C over 0-60 ° C and stability/yr of 0.005 ° C. (Model 5643-R) and Secondary PRT.
- Readout system with an accuracy of 0.0025 ° C at 25 ° C and resolution of 0.0001 ° (Chub E4)

The specifications for the NIST traceable temperature controlled water bath are:

- Deep, mid-range (-10° C to 110 ° C), water bath with a stability specification: ± 0.0008 ° C from 0-25 ° C. (Model 7012)
- Thermistor standard probe with an accuracy specification of 0.0015 ° C over 0-60

° C and stability/yr of 0.005 ° C. (Model 5643-R) and Secondary PRT.
- Readout system with an accuracy of 0.0025 ° C at 25 ° C and resolution of 0.0001 ° (Chub E4)

Calibration of the radiometers and bulk temperatures is performed in a ramp and soak mode where the blackbody or water-bath temperature is increased by a set interval and allowed to soak for several minutes and then the temperature is measured. The measured temperatures are then compared to the standard probe temperatures to derive calibration coefficients for the radiometer or bulk temperature sensors. After calibration the bulk temperature sensors and radiometers have accuracies of ± 0.1 ° C and ± 0.08 ° C respectively.

All data are analyzed using our in-house computer facility. Software developed at this facility includes 150 application programs developed under the TAE-VICAR environment and hosted on UNIX and WINDOWS computers. In addition the facility hosts a variety of commercial image display and analysis software operating under WINDOWS and UNIX. These include the Interactive Display Language (IDL) and Environment for the Visualization of Images (ENVI).

6.0 Current Results

As noted earlier, the Lake Tahoe site was used to validate the radiance at sensor and surface temperature and emissivity whereas the Australian sites were only used to validate the surface temperature and emissivity products.

6.1 Validation of At Sensor Radiance Product from ASTER and MODIS

In order to validate the at-sensor product from ASTER and MODIS the lake skin temperature measured at a given buoy is propagated through the atmosphere using a radiative transfer model to derive at-sensor radiance. The derived at-sensor radiance is then convolved to the instrument system response function. Details of these steps together with the associated errors are described in the earlier sections.

Figure 5 shows a plot of the radiance difference between the predicted (Vicarious) at-sensor radiance and measured (OBC) radiance for MODIS for the period from launch through the end of 2002.

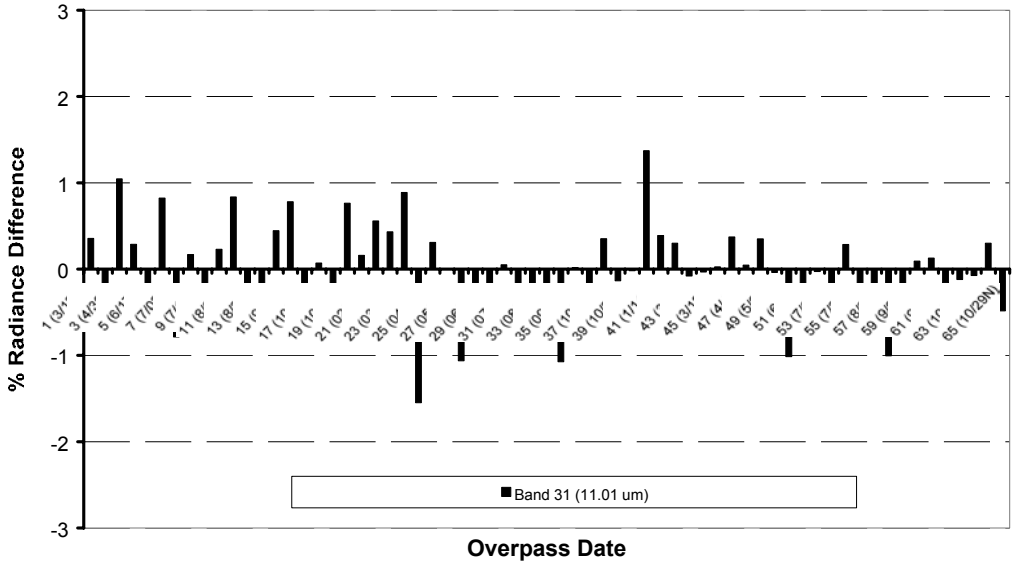

Figure 5 MODIS Terra % Radiance Difference between Vicarious and OBC Derived Radiance for Channel 31 at Lake Tahoe CY2000-2002 ((V-O)/V)*100

During this period ~70 validations were undertaken and on each validation day there were typically 4 matchups (1 per buoy) for a total of 280 independent validations. The validations were undertaken approximately every 16 days and include a day validation and a night validation and cover the temperature range 4-20 º C. The 16 day cycle was centered on the nadir overpass. The original specification for the MODIS instrument required that the absolute calibration of the instrument be at the 1% radiance level. Figure 5 clearly shows that the MODIS instrument has met that specification for Channel 31 for the duration of the mission thus far. If MODIS data are to be used as climate date records it is essential to demonstrate the instrument has met the calibration specification and the periodic calibration accurately compensates for any change in performance of the instrument with time.

A similar analysis was undertaken for the ASTER channels. All the ASTER channels are in the thermal infrared window (8-12 um) and the results for the ASTER channel least affected by the atmosphere (channel 13) are shown in Figure 6.

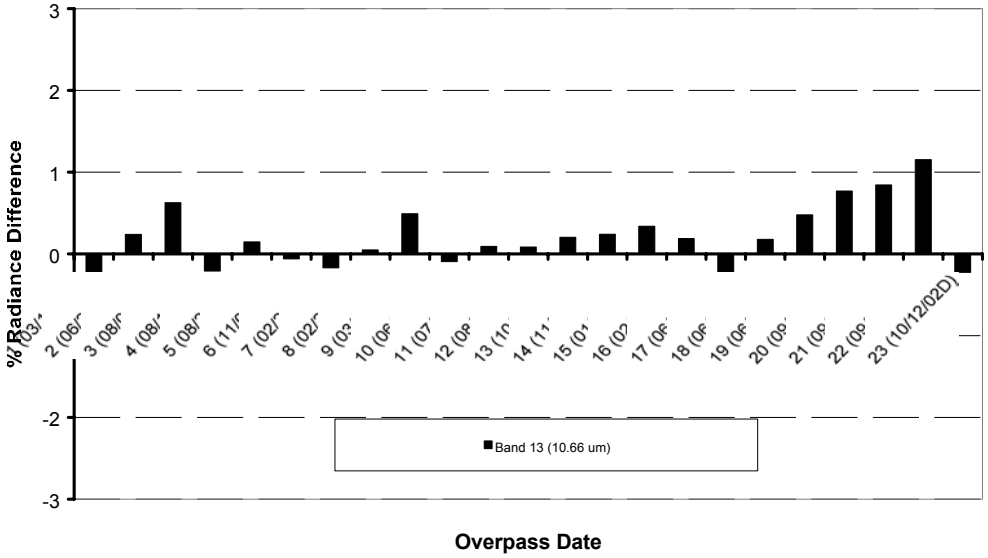

Figure 6 ASTER 3x3 pixel % Radiance Difference between Vicarious and OBC Derived ((V-O)/V)*100.

Examination of this plot indicates that from launch to 7/22/01 (11) the difference between the predicted and measured values was at the level of a few tenths of a percent. Starting around 7/22/01 (11) the difference increased until 6/6/02 (17) when it turned slightly negative the difference then increased until 9/26/02 (22) when it returned to slightly negative values. On 9/26/02 (22) the difference exceeds the 1% level, a change which is equivalent to 0.7K and close to the calibration requirement limit at this wavelength. This increase in radiance error followed by a sharp correction is due to the instrument response degrading with time and being periodically corrected with updated coefficients derived from the onboard blackbody. Updated coefficients are derived every 33 days and the calibration tracks the instrument degradation. Unfortunately although coefficients are derived, the 1B software is only updated if the change exceeds a certain threshold. Even when the threshold has been exceeded it can take several months before the updated coefficients are implemented in the 1B software. In the case above it is the delay in implementing the coefficients that causes the radiance error rather than too few long term calibrations. The ASTER science team is working with the Japanese DAAC to improve this situation and the US science offers a web site to derive a correction factor to account for any delays in the coefficient updates. The problem was identified and illustrated using the Tahoe data and demonstrates how this kind of monitoring is essential if the EOS data are going to be used produce climate records that reflect climate rather than instrument changes.

The validation results can be used to produce a quantitative estimate of the absolute calibration of the MODIS and ASTER channels as shown in Table 7.

Table 7 Summary Validation Results for the In-Flight Validation of Absolute Calibration of MODIS and ASTER "Window" TIR Channels (T=Terra ; A=Aqua)

Sensor	Band and Center (μm)	Preflight Calibration Accuracy Req.	Average of % Radiance Difference (%)	Std Dev of % Radiance Difference (%)	Average of BT Difference (K) (BIAS)	Std. Dev of BT Difference (K) (NEΔT)
MODIS-T	29 (8.53)	< 1%	0.10	0.65	0.05	0.30
MODIS-T	31 (11.02)	< 1%	-0.04	0.55	-0.02	0.33
MODIS-T	32 (12.03)	< 1%	0.11	0.55	0.07	0.36
MODIS-A	29 (8.53)	< 1%	-0.27	0.79	-0.13	0.38
MODIS-A	31 (11.02)	< 1%	-0.07	0.68	-0.04	0.42
MODIS-A	32 (12.03)	< 1%	0.13	0.65	0.09	0.44
ASTER	10 (8.29)	≤ 1K	0.49	0.54	0.23	0.26
ASTER	11 (8.63)	≤ 1K	0.55	0.53	0.27	0.26
ASTER	12 (9.08)	≤ 1K	0.31	0.65	0.33	0.34
ASTER	13 (10.66)	≤ 1K	0.20	0.39	0.12	0.24
ASTER	14 (11.29)	≤ 1K	0.44	0.44	0.28	0.28

The results indicate that the ASTER and MODIS instruments meet the preflight specification, and that the ASTER instrument has a bias due to the correction procedure for the degradation of the instrument as described above. Results are shown for MODIS-Terra and MODIS-Aqua and indicate both systems are well calibrated, although a limited number of MODIS-Aqua validations have been completed. The NEΔT value is a conservative estimate for the band averaged NEΔT of the instrument including any error associated with the vicarious measurements.

6.2 Validation of Surface Products from ASTER and MODIS

Validation of the surface products involves comparison of the geophysical parameter derived from the instrument with the same geophysical parameter measured on the ground.

Figure 7 shows the result from comparing the ASTER surface temperature product (AST08) with the measured skin temperature. Also shown on this figure is the difference between the ground predicted brightness temperature at sensor and the ASTER brightness temperature at sensor (From Figure 6, except brightness temperature rather than radiance). Examination of this Figure indicates that the ASTER surface temperature has a cold bias and superimposed on that cold bias is the "saw tooth" effect due to incomplete removal of the instrument degradation as described in the previous section.

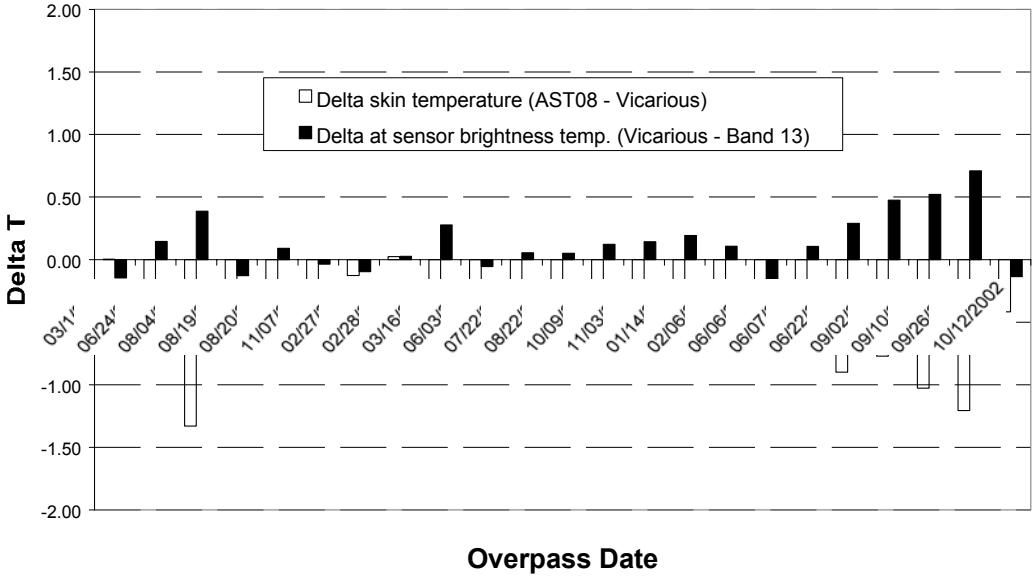

Figure 7 Differences between ASTER Products (AST1B, AST08) and Vicarious Measurements at Lake Tahoe CA/NV CY 2000-2002

One of the validations (08/04/2000) has a very large error caused by the ASTER T-E separation algorithm taking the wrong path and using the coefficients for land rather than the coefficients for water. This problem has been addressed by adjusting the threshold that the algorithm chooses the processing path. This problem arises because the noise characteristics of the surface radiance data used by the T-E product could not be fully determined until after launch. The data from the Tahoe site were used to adjust this threshold to a more appropriate setting. The ASTER T-E separation algorithm is described in Gillespie et al. (1998).

A similar analysis was initially attempted for the MODIS Land Surface Temperature (LST) product (MOD11) but it was discovered that in almost every cloud-free scene surface temperatures were not calculated over water pixels.

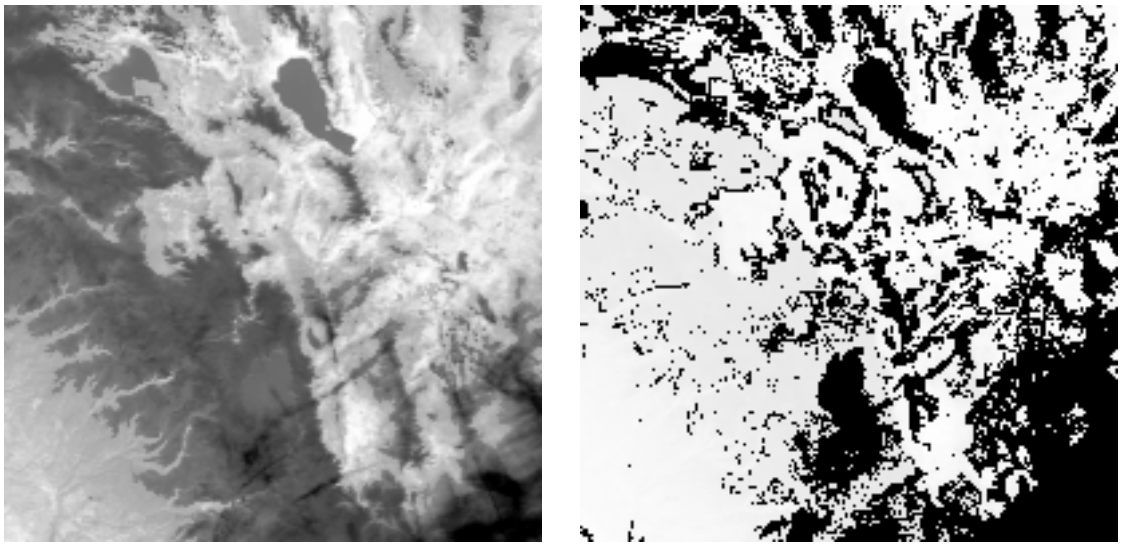

Figure 8 Daytime MODIS scene acquired over Lake Tahoe on 3/12/2000. Image on left is a grayscale brightness temperature image from the band 31 and image on right is the MODIS surface temperature product.

Further investigation determined that the cloud mask product (MOD35) almost always identified inland water, especially at high altitude, as having a less than 99% chance of being cloud free. Only pixels that are identified as having a 99% chance of being cloud free in the MOD35 product are processed with the MOD11 software. This issue was passed on to the MODIS team and the MOD11 software modified such that the surface temperature was calculated for water pixels that were identified as having up to a 66% chance of being cloud free to compensate for the problem with the cloud-mask product. The water pixels were identified from the land/water mask. The results are shown in Figure 9, examination of this figure indicates that surface temperatures calculated using the MODIS LST algorithm over water have a positive bias compared to the field data. This contrasts with results from the ASTER LST algorithm, which have a negative bias, compared with the field data (Figure 7). Both these products are within specification (better than 1 ° C) over this cover type, but clearly the products could be improved to remove these biases.

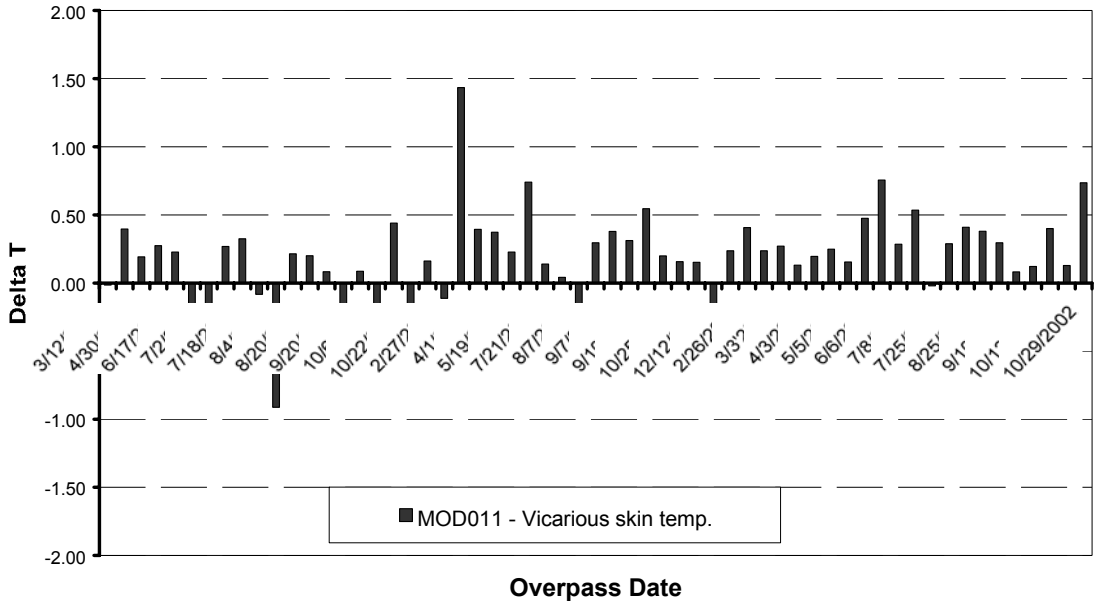

Figure 9 Difference between MODIS LST (MOD11) and Vicarious Measurements at Lake Tahoe CA/NV CY 2000-2002

As noted earlier, this effort includes activities at several sites in order to validate the derived surface product over a range of cover types and atmospheric conditions. The Uardry test site was selected to validate data from the temperature and emissivity retrieval algorithms of ASTER and MODIS over grassland. Initial examination of the MODIS data revealed that, like the Tahoe site, the LST product from MODIS had not been calculated over the Uardry site. Further research indicated that this was caused by much of the interior of Australia being perpetually identified as having a less than 99% chance of being cloud-free in the cloud mask and as a result the LST product was not calculated. This problem was passed onto the MODIS team and it was determined that up to and including Collection 3 of MODIS data much of the interior of Australia was not consistently classified as arid lands. The MODIS cloud mask algorithm relies on a ecosystem map to determine the initial surface parameters for calculating the cloud mask. MODIS data are arranged in collections which mark a major reprocessing of the data. Because of this incorrect classification, the cloud mask clear-sky restoral test was not run in the region and the surface was incorrectly identified as cloud. In Collection 4 processing, a clear-sky restoral test for all snow-free land surfaces, was implemented thereby avoiding this ecosystem classification problems. The figure below shows the cloud mask for the **same** image in Collection 3 and Collection 4.

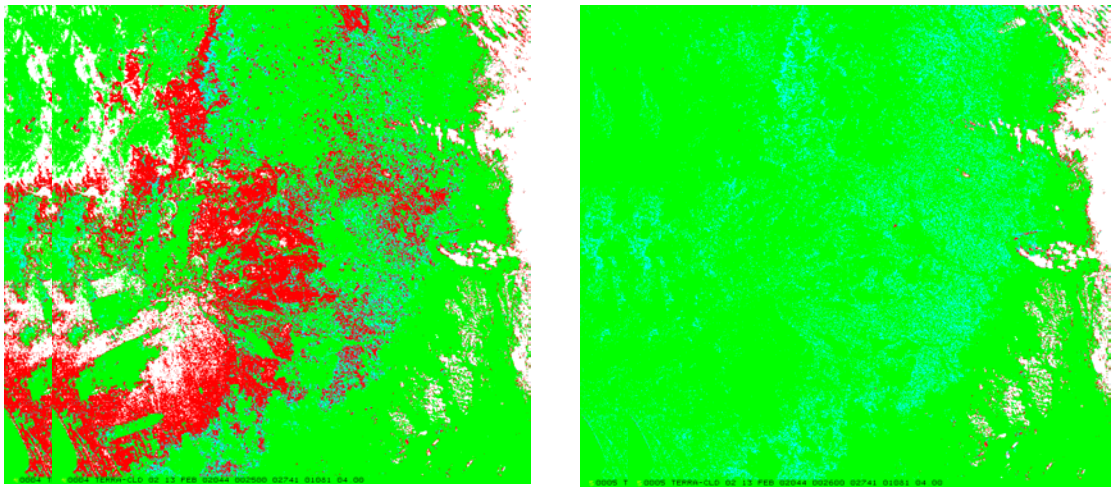

Figure 10 Left image – Cloud Mask for Uardry region using Collection 3 software. Pixels colored green were identified as 99% cloud-free by the cloud mask algorithm and processed to surface temperature. Cloud Mask for Uardry region (same input scene as left image) processed using the Collection 4 software.

Collection 4 reprocessing for the land products began in late 2002 and is continuing today. Results from Uardry for the Collection 4 data reprocessed thus far as well as Collection 3 scenes not affected by the cloud masking problem are summarized in the table below:

	Predicted (MODIS) - Measured		
Instrument	Field Brightness Temperature	Field Kinetic Temperature Green Grass	Field Kinetic Temperature Dry Grass
MOD11	-1.41	-1.91	-3.56
AST08	-1.02	-1.71	-3.17

Table 8 Average bias Between Instrument Derived Surface Temperature and Measured Surface Temperature for the Uardry Field Site.

Table 8 shows the results if the radiometers were viewing green grass or if they were viewing dry grass. The results for both surface types are shown to provide an indication of the size of the difference between surface types, although the site is typically green. The procedure for deriving the surface kinetic temperature is the same procedure used for the Tahoe site except the emissivity of grass is used instead of water. Examination of Table 8 indicates there is a bias between the LST products exceeds the specified error of 1 ° C. The results also show that in order for the LST to meet the specification the site must have an emissivity that is higher than green grass, which is clearly unrealistic. There are clear differences between the MODIS and ASTER algorithms and this can be illustrated by looking at the ASTER derived emissivity for the site in Figure 11. Examination of this figure indicates that, according to ASTER the emissivity for the site is decreasing over time.

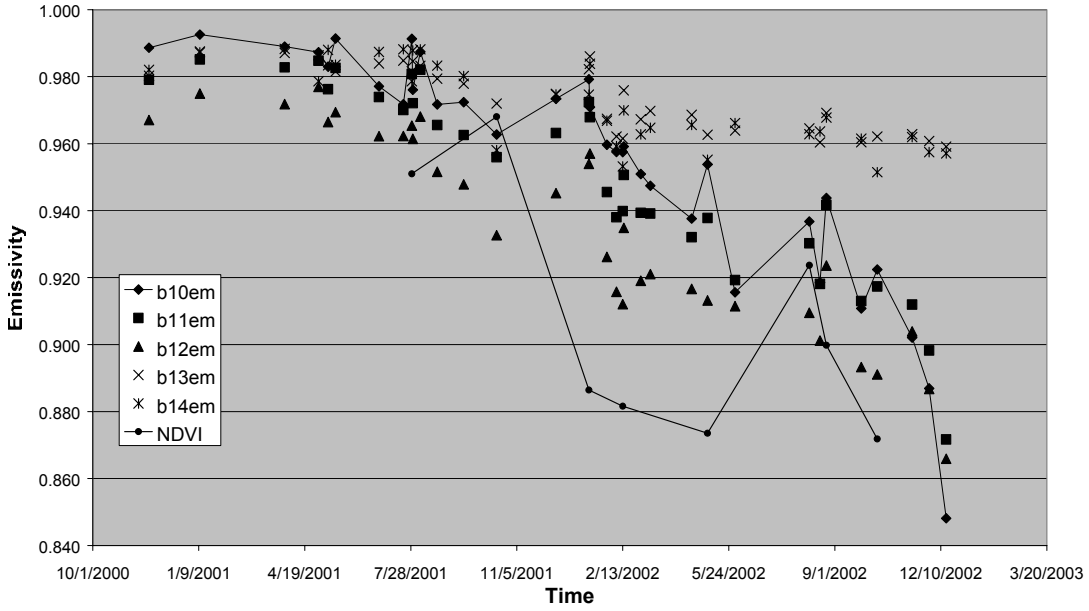

Figure 11 Change in emissivity over time at the Uardy site.

This decline is believed to be real and the result of a drought. In the MODIS LST product the surface emissivity is assumed to be constant and does not account for this change which may explain the better result for ASTER. It should be noted the wavelength range over which the MODIS algorithm assumes the emissivity is constant is covered by ASTER channels 13 and 14 where the change is less than at shorter wavelengths.

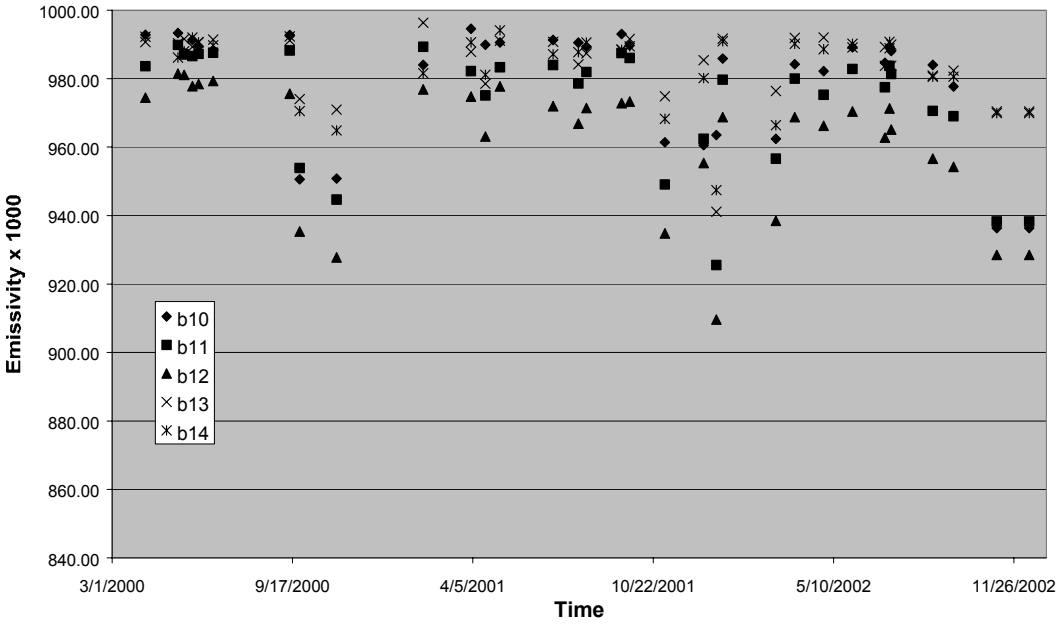

Figure 12 Change in emissivity at the Amburla site.

Figure 12 shows the change in the ASTER emissivity product over time for the Amburla site. At this site there are three pronounced changes in emissivity associated with dry season when the soil is exposed and the vegetation dies off. This illustrates the difficulty of using an algorithm that assumes the emissivity is constant based on an a priori classification of the surface into a limited number of cover types as used with the MODIS and NPOESS LST algorithms. Although considerable progress has been made in validating the LST algorithms of MODIS and ASTER at the Australian sites further work is needed to fully understand the validation data.

Publications and Media (this project)

Hook, S. J. In Flight Validation of Thermal Infrared Data over Land. European Symposium on Remote Sensing: SENSORS, SYSTEMS AND NEXT GENERATION SATELLITES IV, Barcelona, Spain, September 21-25, 1998. (Abstract).

Hook, S. J., Schladow, G., Abtahi, A. F. Prata and B. Richards. In-Flight Validation of Remotely Sensed Thermal Infrared Data for Hydrological Applications. American Geophyscial Union, September 1999, San Francisco. (Abstract)

Hook, S. J., G. Schladow, A. Abtahi, F. Prata, B. Richards and S. Palmarsson. Validation of ASTER and MODIS Thermal Infrared Products. Sixth International Conference Remote Sensing for Marine and Coastal Environments. Charleston, South Carolina, May 1-3 2000. (Abstract)

Hook, S. J., Myers, J. J., Thome, K. J., Fitzgerald, M. and A. B. Kahle, 2001. The MODIS/ASTER Airborne Simulator (MASTER) – A New Instrument for Earth Science Studies. *Remote Sensing of Environment*, vol. 76, Issue 1, pp. 93-102.

Hook, S. J. Thome, K. J., Myers J. J. and M. Fitzgerald. In Flight Validation of MASTER Data – A Necessity for Quantitative Geologic Mapping. Fourteenth International Conference and Workshops on Applied Geologic Remote Sensing, Las Vegas, Nevada, November 6-8, 2000. (Abstract)

Hook, S. and F. Prata. Land Surface Temperature Measured by ASTER and MODIS - First Results. European Geophysical Society, 26th General Assembly, Nice, France, March 25-30 2001. (Abstract)

Hook, S. J., Prata, F. J., Abtahi, A., Alley, R. E., Richards, R. C. and S. G. Schladow Cross Validation Of Thermal Infrared Remotely Sensed Data In-Flight Using An Automated Validation Site – Lake Tahoe CA/NV, USA. 1st International Symposium on Recent Advances in Quantitative Remote Sensing, Valencia, Spain, Sept. 16-20, 2002. (Abstract)

Barsi, J. A., Schott, J. R., Palluconi, F. D., Helder, D. L., Hook, S. J., Markhum, B. L., Chander, G., and E. M. O'Donnell, 2003. Landsat TM and ETM+ Thermal Band Calibration. *Canadian Journal of Remote Sensing*, Vol. 29, No. 2.

Hook, S. J., Prata A. J., Alley, R. E., Abtahi, A., Richards, R. C., Schladow, S. G. and S. Ó. Pálmarsson, 2003 Retrieval of Lake Bulk-and Skin-Temperatures using Along Track Scanning Radiometer (ATSR) Data: A Case Study using Lake Tahoe, CA. *Journal of Atmospheric and Oceanic Technology*, Vol. 20, No. 2, pp 534-548.

Barton, I. J, Minnett, P. J., K. A. Maillet, Donlon, C. J., Hook, S. J., Jessup, A. T and T. J. Nightingale, 2002. The Miami2001 infrared radiometer calibration and inter-comparison: 2. Ship board results. Accepted Journal of Atmospheric and Oceanic Technology.

Rice, J. P., Butler, J. J., Johnson, B. C., Minnett, P. J., Maillet, K. A., Nightingale, S. J. Hook, A. Abtahi, C. J. Donlon and I. J. Barton 2002. The Miami2001 Infrared Radiometer Calibration and Intercomparison: 1. Laboratory Characterization of Blackbody Targets. Accepted Journal of Atmospheric and Oceanic Technology.

Tahoe World January 13 2000. 1.3 billion satellite links Tahoe to NASA ***By Shannon Darling, Tahoe World Staff.***

Tahoe World March 10, 2000. NASA rafts await satellite data ***By Shannon Darling, Tahoe World Staff.***

References

Barsi, J. A., Schott, J. R., Palluconi, F. D., Helder, D. L., Hook, S. J., Markhum, B. L., Chander, G., and E. M. O'Donnell, 2003. Landsat TM and ETM+ Thermal Band Calibration. *Canadian Journal of Remote Sensing*, Vol. 29, No. 2.

Barton, I. J., Minnett, P. J., Maillet, K. A., Donlon, C. J., Hook, S. J., Jessup, A. T. and T. J. Nightingale, 2002. The Miami2001 infrared radiometer calibration and inter-comparison: Ship comparisons. *Submitted* Journal of Atmospheric and Oceanic Technology.

Berk, A., L. S. Bernstein and D. C. Robertson, 1989. MODTRAN: A Moderate Resolution Model for LOWTRAN 7. *Tech. Rep. GL-TR-89-0122,* Geophys. Lab., Bedford, Mass.

Gillespie, A., Rokugawa, S. Matsunaga, T., Cothern, S, Hook, S. and A. Kahle, 1998. A Temperature and Emissivity Separation Algorithm for Advanced Spaceborne Thermal Emission and Reflectance Radiometer (ASTER) Images. IEEE Transactions on Geoscience and Remote Sensing, vol. 36 pp. 1113-1126.

Gillespie, A., Gillespie, A., Rokugawa, S. Matsunaga, T., Cothern, S, Hook, S. and A. Kahle, 1999. The ASTER Temperature/Emissivity Separation Algorithm Theoretical Basis Document (ATBD-AST-03). http://eospso.gsfc.nasa.gov/eos_homepage/for_scientists/atbd/docs/ASTER/atbd-ast-03.pdf.

Hook, S. J., and K. Okada, 1996. In-flight Wavelength Correction of Thermal Infrared Multispectral Scanner (TIMS) Data acquired from the ER-2. *IEEE Geoscience and Remote Sensing*, vol. 34, pp 179-188.

Hook, S. J., and A. B. Kahle, 1996. The micro Fourier Transform Interferometer (μFTIR) - A New Field Spectrometer for Acquisition of Infrared Data of Natural Surfaces. *Remote Sens. Environ*. vol. 56, pp. 172-181.

Hook, S. J., Prata A. J., Alley, R. E., Abtahi, A., Richards, R. C., Schladow, S. G. and S. Ó. Pálmarsson, 2003 Retrieval of Lake Bulk-and Skin-Temperatures using Along Track Scanning Radiometer (ATSR) Data: A Case Study using Lake Tahoe, CA. *Journal of Atmospheric and Oceanic Technology,* vol. 20, No. 2, pp 534-548.

Palluconi, F., Hoover, G, Alley, R, Jentoft-Nilsen, M. and T. Thompson, 1999. An Atmospheric Correction Method for ASTER Thermal Radiometery over Land (ATBD-AST-05). http://eospso.gsfc.nasa.gov/eos_homepage/for_scientists/atbd/docs/ASTER/atbd-ast-05.pdf.

Prata, A. J. 1994, Land surface temperatures derived from AVHRR and ATSR. II: Experimental results and validation of AVHRR algorithms, *J. Geophys. Res*., vol. 99, pp. 13,025 -13,058.

Rice, J. P., Butler, J. J., Johnson, B. C., Minnett, P. J., Maillet, K. A., Nightingale, S. J. Hook, A. Abtahi, C. J. Donlon and I. J. Barton 2002. The Miami2001 Infrared Radiometer Calibration and Intercomparison: 1. Laboratory Characterization of Blackbody Targets. Submitted Journal of Atmospheric and Oceanic Technology.

Schott, J. R., and W. J. Volchok, 1985. Thematic Mapper Thermal Infrared Calibration. *Photogrammetric Engineering and Remote Sensing*, vol. 51, pp. 1351-1357.

Schott, J. R., 1989. Image Processing of Thermal Infrared Images. *Photogrammetric Engineering and Remote Sensing*, vol. 55, pp. 1311-1321.

Walton, C., 1988, Nonlinear multichannel algorithms for estimating sea surface temperature with AVHRR satellite data, *J. Appl. Meteorol*., vol. 27, pp. 115 - 124.

Wu, X. Q. and W. L. Smith, 1997. Emissivity of rough sea surface for 8-13 um: Modeling and Verification. Applied Optics, vol. 36 pp. 2609-2619.

Wan, Z, 1999. MODIS Land-Surface Temperature Algorithm Theoretical Basis Document (LST ATBD) Version 3.3. http://modis.gsfc.nasa.gov/data/atbd/atbd_mod11.pdf.

Collaborations

Strong collaborations have been established with the EOS instrument teams (ASTER, MODIS and Landsat) as well as other instruments such as Multispectral Thermal Imager developed by the Department of Energy and Along Track Scanning Radiometer developed by the Rutherford Appleton Laboratory and flown on a European platform.

Archiving

A web site has been established which is the primary mechanism for disseminating information. All data on the site are backed up as part of the main ASTER archive over the network and also locally on a nightly basis. In addition the MODIS instrument team designated Lake Tahoe an EOS Core Site in CY2000, primarily thanks to Jeff Morisette on the MODIS land validation team. As a result of this designation a large amount of data associated with the site is being made available online. Efforts are also being made to include the validation information at this site:

http://modis-land.gsfc.nasa.gov/val/

Note: Both Lake Tahoe and Uardy are now designated as EOS Core Sites.

WebPages

http://laketahoe.jpl.nasa.gov/
http://shookweb.jpl.nasa.gov/validation
http://modis-land.gsfc.nasa.gov/val/
http://blt.wr.usgs.gov/